




On fractional-order symmetric oscillator with offset-boosting control*

Changjin Xu^{a,b} , Mati ur Rahman^{c,1} , Dumitru Baleanu^{d,e} 

^aGuizhou Key Laboratory of Economics System Simulation,
Guizhou University of Finance and Economics,
Guiyang 550025, China

^bGuizhou Key Laboratory of Big Data Statistical Analysis,
Guiyang 550025, China

^cSchool of Mathematical Science,
Shanghai Jiao Tong University
Shanghai, China
mati-maths_374@sjtu.edu.cn

^dDepartment of Mathematics, Cankaya University,
06530 Balgat, Ankara, Turkey

^eInstitute of Space Sciences,
R76900 Magurele-Bucharest, Romania

Received: February 25, 2022 / Revised: June 24, 2022 / Published online: July 19, 2022

Abstract. This article analyzes the dynamical evolution of a three-dimensional symmetric oscillator with a fractional Caputo operator. The dynamical properties of the considered model such as equilibria and its stability are also presented. The existence results and uniqueness of solutions for the suggested model are analyzed using the tools from fixed point theory. The symmetric oscillator is analyzed numerically and graphically with various fractional orders. It is observed that the fractional operator has a significant impact on the evolution of the oscillator dynamics showing that the system has a limit-cycle attractor. Offset-boosting control phenomena in the system are also studied with different orders and parameters.

Keywords: symmetric oscillator, Caputo operator, limit-cycle attractor, offset boosting.

1 Introduction

Fractional calculus (FC) has been widely used in a variety of fields of science. Many different definitions have been introduced in the literature based on this level of importance.

*This research was supported by Guizhou Key Laboratory of Big Data Statistical Analysis grant No. [2019] 5103.

¹Corresponding author.

The fractional operator of Caputo is probably the most important one in fractional calculus [20, 22]. The nonlocal feature of fractional-order derivatives is demonstrated to be a significant component in the huge variety of fractional calculus implementations [8, 25, 31]. The integer-order derivatives of a function at a specific point may be estimated using neighboring data, while the fractional derivative requires the complete history beginning at the origin. This nonlocality of the fractional derivative (FD) is important in modeling storage and hereditary aspects in the system [27]. As a consequence, models using FD are more authentic than models using the integer order. The second benefit of the FD is that it can simulate intermediary operations. Because the operations are intermediate, the integer-order derivatives cannot reflect the true occurrences in various physical situations such as fluid movement in porous media. Since analytical approaches are incapable of solving much fractional-order complex behavior, a variety of algorithms has been introduced to obtain an approximate solution to fractional-order systems [3, 23].

There are several fractional-order operators that have been presented in FC, including Caputo, Caputo–Fabrizio and Atangana–Baleanu in Caputo’s sense [2, 4]. These operators are very advantageous because of the complexity of fractional nonlinear differential equations (FNDEs). The integer-order operators are not able to study such equations in order to get explicit solutions. Due to this disadvantage of the integer-order operators, one needs a best numerical method to get the coefficients of the series solutions of FNDEs [24]. The Caputo operator is utilized widely in different problems in applied sciences, but this operator has a singular kernel. To generalize this, Caputo and Fabrizio introduced a nonsingular fractional operator using an exponential-type kernel. Similarly, another form of nonsingular and nonlocal fractional operator, known as Atangana–Baleanu fractional operator, produces efficient results due to the nonlocal and nonsingular kernel [11].

Differential equations (DEs) have become an essential field of mathematics that is being used to describe several physical phenomena. Complex systems are one of the most important and constantly increasing areas that makes extensive use of DEs. The dynamical system can characterize every point in dimensional space across time. When the mathematical system is a real-world issue throughout in the form of a dynamic system, its state at any moment t may be forecasted. In the analysis and prediction of such systems, the fractional-order calculus has been observed to be a useful tool for comprehending complex dynamical systems having nonlinear properties [17, 18].

In 1963, Lorenz presented chaos for the first time [16]. Since then, chaos has piqued the interest of several scientists and scientific communities around the world, and it has been effectively implemented in recent decades, mainly, in the field of communication channels. Chaos has played an important part in control applications such as regulating irregular behavior in devices and systems [5], communication privacy, and synchronization of same or separate systems resulting in data encryption, chaos spectrum radio, and secure communications [6]. A chaos system is a set of differential equations in which the solutions to two relatively comparable situations change dramatically at any given moment. For the aforementioned reasons, several chaotic systems have been created to induce chaos. Attractors, which are a collection of invariant points in dimensional space, are produced by these systems.

Although the majority of chaotic systems are of integer order, it has been revealed that fractional-order chaotic systems, due to their dynamic nature, are superior at realizing actual things. As compared to the integer-order systems, fractional chaotic models are better suitable for modeling nonlinear systems in nature. Nonlocality characterizes fractional-order systems since their future state is governed not only by their present state but also by the circumstances of their prior states. Because fractional calculus can increase the complexity and precision of chaos, researchers are interested in fractional-order multi-wing chaotic systems. Also, many researchers around the globe have studied a wide range of chaotic systems with fractional-order operators, where they found this area as an important tool to analyze complexities present in the system [15, 26, 30].

Hidden chaotic attractors and hidden periodic oscillations have been investigated in drilling systems [13], phase-locked loops [12], and in aviation control systems [13]. Hidden attractors have an attraction basin that is not related to any neighboring regions of equilibrium, which indicates that they are not self-excited attractors. Integer-order derivatives are used extensively in the realization of hidden attractors. Noninteger derivatives, on the other hand, can be used to find hidden attractors in a chaotic system. The study of hidden attractors in fractional-order systems is the most effective technique to go further into a fascinating and important new subject. However, there is less amount of research present in this area, which makes it an interesting field for research to realize the hidden attractors with fractional derivatives [1]. As a result, the study of hidden attractors in noninteger-order systems is important for understanding this fascinating area. Fractional-order systems with hidden attractors having one equilibrium [9], no equilibria [21], a line or surfaces of equilibria [10], and even fractional-order hyper-chaotic systems [29] have been introduced in literature. Also, different families of hidden attractors have been studied in [19].

Motivated from these works, we study a three-dimensional oscillator that is chaotic with a fractional-order power law. We study the hidden attractors present in the system with specific values of the control parameters. The numerical algorithm used for the solution has many advantages. For the numerical analysis, we use the method, which is consistent, stable, and convergent [7]. Here we consider the 3D symmetric oscillator [28]

$$\begin{aligned}\frac{d\mathcal{X}}{dt} &= \mathcal{Y}\mathcal{Z}, \\ \frac{d\mathcal{Y}}{dt} &= \mathcal{X}^3 - \mathcal{Y}^3, \\ \frac{d\mathcal{Z}}{dt} &= \Omega\mathcal{X}^2 + \Pi\mathcal{Y}^2 - \eta\mathcal{X}\mathcal{Y}.\end{aligned}\tag{1}$$

For the dimensional consistency, we have replaced d/dt in system (1) with $1/(\kappa^{1-e})$. After simplification, we obtain the considered model in Caputo fractional derivative sense as

$$\begin{aligned}{}^c D_t^e \mathcal{X}(t) &= \Xi\mathcal{Y}\mathcal{Z} \\ {}^c D_t^e \mathcal{Y}(t) &= \Xi\mathcal{X}^3 - \Xi\mathcal{Y}^3 \\ {}^c D_t^e \mathcal{Z}(t) &= \Omega_\kappa\mathcal{X}^2 + \Pi_\kappa\mathcal{Y}^2 - \eta_\kappa\mathcal{X}\mathcal{Y}.\end{aligned}\tag{2}$$

For the offset-boosting control, we consider system (2) in the following form by introducing \mathcal{Y} in its first state variable:

$$\begin{aligned} {}^c D_t^\varrho \mathcal{X}(t) &= \Xi \mathcal{Y}(\mathcal{Y} + \mathcal{Z}), \\ {}^c D_t^\varrho \mathcal{Y}(t) &= \Xi \mathcal{X}^3 - \Xi \mathcal{Y}^3, \\ {}^c D_t^\varrho \mathcal{Z}(t) &= \Omega_\kappa \mathcal{X}^2 + \Pi_\kappa \mathcal{Y}^2 - \eta_\kappa \mathcal{X} \mathcal{Y}. \end{aligned} \tag{3}$$

In models (2) and (3), we have $\Xi = \kappa^{\varrho-1}$, $\Omega_\kappa = \Omega \kappa^{\varrho-1}$, $\Pi_\kappa = \Pi \kappa^{\varrho-1}$, and $\eta_\kappa = \eta \kappa^{\varrho-1}$.

2 Preliminaries

Some important and helpful definitions, lemmas are stated below.

Definition 1. (See [22].) Let a function $g(t) \in L([0, 1], \mathbb{R})$, then the Riemann–Liouville fractional integral of order $0 \leq \alpha < 1$ is defined as follows:

$$I_t^\alpha g(t) = \frac{1}{\Gamma(\alpha)} \int_0^t \frac{g(\xi)}{(t - \xi)^{1-\alpha}} d\xi, \quad t > 0.$$

Definition 2. (See [22].) Let a function $g(t) \in C[0, 1]$, then the Capute fractional derivative of order $0 \leq \alpha < 1$ is defined as follows:

$${}^c D_t^\alpha g(t) = \frac{1}{\Gamma(1 - \alpha)} \int_0^t \frac{g'(\xi)}{(t - \xi)^\alpha} d\xi, \quad t > 0.$$

Lemma 1. (See [22].) *The given results satisfy the problems related to noninteger order*

$$\begin{aligned} {}^c D_t^\alpha g(t) &= W(t), \quad 0 \leq \alpha < 1, \\ g(0) &= g_0, \quad g(t) = g_0 + \frac{1}{\Gamma(\alpha)} \int_0^t (t - \gamma)^{\alpha-1} W(\gamma) d\gamma. \end{aligned}$$

3 Equilibria and its stability

Here we calculate the equilibrium points of system (2). For obtaining so, we equate all the equations in system (2) to zero. So we get

$$\begin{aligned} \Xi \mathcal{Y} \mathcal{Z} &= 0, \\ \Xi \mathcal{X}^3 - \Xi \mathcal{Y}^3 &= 0, \\ \Omega_\kappa \mathcal{X}^2 + \Pi_\kappa \mathcal{Y}^2 - \eta_\kappa \mathcal{X} \mathcal{Y} &= 0. \end{aligned} \tag{4}$$

After solving Eq. (4), we get $E = (0, 0, \Xi Z)$. From Eq.(4) we see that the system has line of equilibria. The Jacobian of the model is as follows:

$$J = \begin{bmatrix} 0 & \Xi Z & 0 \\ 0 & 0 & 0 \\ 0 & 0 & 0 \end{bmatrix}.$$

The characteristic equation of J is $\mathcal{L}^3 = 0$, where the eigenvalue is $\mathcal{L} = 0$, which shows that the given system is unstable.

4 Bifurcation analysis

The bifurcation exhibits a topological or qualitative shift by gradually changing the bifurcation parameter during the evolution of a dynamical system. A bifurcation diagram can show if a limit cycle, periodic orbit, or chaotic orbit is present. Through a parametric range, it provides a graphical representation of the system’s solutions. To analyze the bifurcations for the suggested system (3), we consider the parameter η with specific interval versus system state variable $\mathcal{X}(t)$ presented in Fig. 1. The time considered here

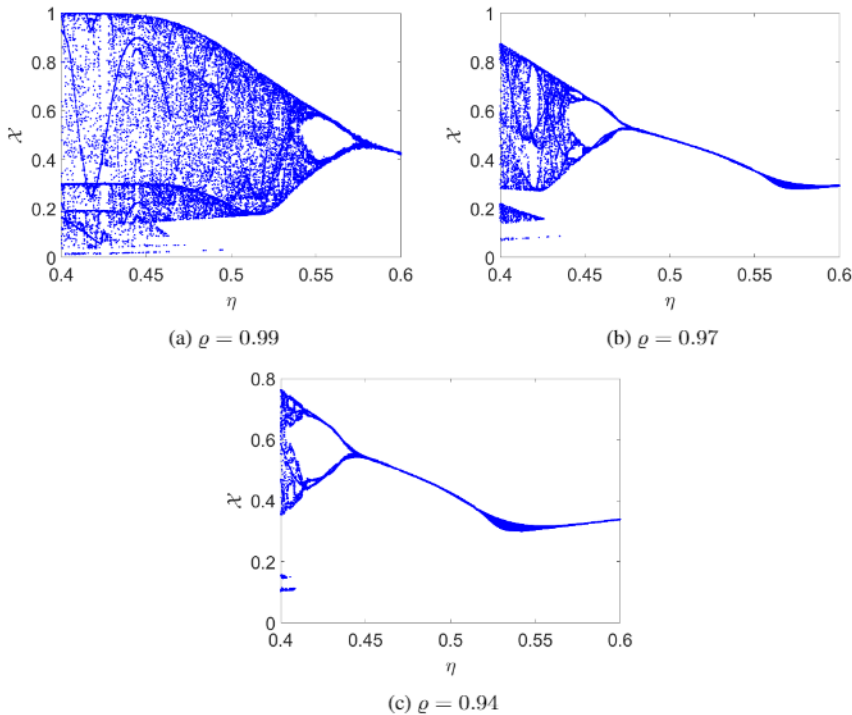


Figure 1. The behavior of state variables \mathcal{X}, \mathcal{Y} of system (2) with varying fractional order ρ .

is 100 with $h = 0.001$, and initial conditions are $\mathcal{X} = 0.1$, $\mathcal{Y} = 0.1$, and $\mathcal{Z} = 0.1$. The inverse period-doubling bifurcation is observed in the figure at $\eta = 0.57$ and $\varrho = 0.99$, also chaos is observed when $\eta < 0.55$. Furthermore, it can be seen that the chaos in the system reduces with decreasing the fractional order and shows that there is a limit cycle orbit in the system, which can be observed in Fig. 1(c).

5 Existence theory

The existence together with the uniqueness for the solution of a dynamical system is necessary. Therefore, here we study the existence as well as the uniqueness of the solutions to the considered systems with fractional order. For this, we use the tools from the fixed point theory. For the sake of convenience, consider system (3) in the form

$$\begin{aligned} {}^c D_t^\varrho \mathcal{X}(t) &= \Lambda_1(t, \mathcal{X}, \mathcal{Y}, \mathcal{Z}), \\ {}^c D_t^\varrho \mathcal{Y}(t) &= \Lambda_2(t, \mathcal{X}, \mathcal{Y}, \mathcal{Z}), \\ {}^c D_t^\varrho \mathcal{Z}(t) &= \Lambda_3(t, \mathcal{X}, \mathcal{Y}, \mathcal{Z}) \end{aligned}$$

for

$$\begin{aligned} \mathfrak{G}_1(t, \mathcal{X}, \mathcal{Y}, \mathcal{Z}) &= \Xi \mathcal{X} \mathcal{Y}, \\ \mathfrak{G}_2(t, \mathcal{X}, \mathcal{Y}, \mathcal{Z}) &= \Xi \mathcal{X}^3 - \Xi \mathcal{Y}^3, \\ \mathfrak{G}_3(t, \mathcal{X}, \mathcal{Y}, \mathcal{Z}) &= \Omega_\kappa \mathcal{X}^2 + \Pi_\kappa \mathcal{Y}^2 - \eta_\kappa \mathcal{X} \mathcal{Y}. \end{aligned}$$

Consider system (2) in the form

$$\begin{aligned} {}^c D_t^\varrho (\gamma(t)) &= \Psi(t, \gamma(t)), \\ \gamma(0) &= \gamma_0 \geq 0, \end{aligned} \tag{5}$$

where

$$\begin{aligned} \gamma(t) &= (\mathcal{X}, \mathcal{Y}, \mathcal{Z})^T, \quad \gamma_0 = (\mathcal{X}(0), \mathcal{Y}(0), \mathcal{Z}(0))^T, \\ \Psi(t, \gamma(t)) &= (\mathfrak{G}_i(t, \mathcal{X}, \mathcal{Y}, \mathcal{Z}))^T, \quad i = 1, 2, 3, \end{aligned}$$

here ‘‘T’’ denote the transpose of a matrix. Also, with the use of Lemma 1, the solution to Eq. (5) can be expressed

$$\gamma(t) = \gamma_0 + \frac{1}{\Gamma(\varrho)} \int_0^t (t - \wp)^{\varrho-1} \Psi(\wp, \gamma(\wp)) \, d\wp.$$

Let us define Banach space $B = L^4$ with the norm $\|\gamma\| = \sup_{t \in [0, b]} |\gamma(t)|$. Let us define the operator $\Theta : B \rightarrow B$ as

$$\Theta[\gamma(t)] = \gamma_0 + \frac{1}{\Gamma(\varrho)} \int_0^t (t - \wp)^{\varrho-1} \Psi(\wp, \gamma(\wp)) \, d\wp.$$

Consider that $\gamma(t, \wp(t))$ satisfy the growth and Lipschitz conditions as

(C1) There exists the constants $M_\Psi, C_\Psi > 0$ such that

$$|\Psi(t, \gamma(t))| \leq M_\Psi + C_\Psi |\gamma|, \quad t \in [0, b].$$

(C2) There exist a constant $L_\Psi > 0$ such that for each $\gamma_1, \gamma_2 \in C(\mathbb{J}, R)$,

$$|\Psi(t, \gamma_1(t)) - \Psi(t, \gamma_2(t))| \leq L_\Psi |\gamma_1(t) - \gamma_2(t)|.$$

For the uniqueness of the solution of system (2), we make use of the following lemma and theorems.

Lemma 2. *If B represent a Banach space and $\Theta : B \rightarrow B$ be continuous completely such that $X_\varrho = \{\gamma \in B : \gamma = \eta\Theta\gamma, \eta \in [0, 1]\}$ is bounded, then there exists at least one root in Θ .*

Theorem 1. *Suppose (C1) holds, and let $\Psi : [0, b] \times B \rightarrow R$ be a continuous function. Then system (2) has at least one solution.*

Proof. Suppose that $X_\varrho = \{\gamma \in B : \|\gamma\| \leq \varrho\}$. Here $X_\varrho \neq \emptyset$ is closed convex subset of B. For the continuity of Θ , consider $\{\gamma_n\}$, a sequence in X_ϱ , such that $\gamma_n \rightarrow \gamma$ as $n \rightarrow \infty$. Suppose, for any $t \in [0, b]$, one can have

$$\begin{aligned} \|\Theta[\gamma_n] - \Theta[\gamma]\| &= \sup_{t \in [0, b]} |\Theta[\gamma_n(t)] - \Theta[\gamma(t)]| \\ &= \sup_{t \in [0, b]} \left| \int_0^t \frac{(t - \wp)^{\varrho-1}}{\Gamma(\varrho)} [\Psi(\wp, \gamma_n(\wp)) - \Psi(\wp, \gamma(\wp))] d\wp \right| \\ &\leq \frac{L_\Psi}{\Gamma(\varrho)} \sup_{t \in [0, b]} \int_0^t (t - \wp)^{\varrho-1} |\gamma_n(\wp) - \gamma(\wp)| d\wp. \end{aligned}$$

As Ψ is continuous, so by Lebesgue dominant convergence theorem we have

$$\|\Theta[\gamma_n] - \Theta[\gamma]\| \rightarrow 0 \quad \text{as } n \rightarrow \infty.$$

Hence, Θ is continuous. Moreover to show that Θ is bounded or $\Theta(X_\varrho) \subset X_\varrho$ take

$$\begin{aligned} \|\Theta[\gamma]\| &= \sup_{t \in [0, b]} |\Theta[\gamma(t)]| = \sup_{t \in [0, b]} \left| \int_0^t \frac{(t - \wp)^{\varrho-1}}{\Gamma(\varrho)} \Psi(\wp, \gamma(\wp)) d\wp \right| \\ &\leq \frac{b^\varrho}{\Gamma(\varrho + 1)} [M_\Psi + C_\Psi \|\gamma\|] \leq \rho. \end{aligned}$$

Since $\|\Theta[\gamma]\| \leq \rho$, it shows that Θ is bounded. Now to study that Θ is compact, we have to show that Θ is equicontinuous operator. For this, let us take $t_1, t_2 \in [0, b]$, so we have

$$\begin{aligned} &|\Theta[\gamma(t_2)] - \Theta[\gamma(t_1)]| \\ &\leq \int_0^{t_1} \frac{1}{\Gamma(\varrho)} [(t_1 - \wp)^{\varrho-1} - (t_2 - \wp)^{\varrho-1}] |\Psi(\wp, \gamma(\wp))| d\wp \\ &\quad + \int_{t_1}^{t_2} (t_2 - \wp)^{\varrho-1} |\Psi(\wp, \gamma(\wp))| d\wp \\ &\leq \frac{(M_\Psi + C_\Psi \varrho)}{\Gamma(\varrho)} \left[\int_0^{t_1} [(t_1 - \wp)^{\varrho-1} - (t_2 - \wp)^{\varrho-1}] d\wp + \int_{t_1}^{t_2} (t_2 - \wp)^{\varrho-1} d\wp \right] \\ &\leq \frac{(M_\Psi + C_\Psi \varrho)}{\Gamma(\varrho + 1)} (t_1^\varrho - t_2^\varrho + (t_2 - t_1)^\varrho). \end{aligned}$$

Hence, we see that $\|\Theta[\gamma(t_2)] - \Theta[\gamma(t_1)]\| \rightarrow 0$ as $t_2 \rightarrow t_1$, which shows that Θ is equicontinuous. Using Arzelà–Ascoli theorem, the operator Θ has at least one fixed point. Hence, the considered system has at least single solution. \square

Next, we need to show the uniqueness of the solution to system (2). For this, we make use of the following theorem.

Theorem 2. *Let (C2) holds, then the solution of the considered system (2) is unique if $L_\Psi \sigma < 1$, where*

$$\sigma = \frac{a^\varrho}{\Gamma(\varrho + 1)}.$$

Proof. For the proof of the above theorem, let $\gamma_1, \gamma_2 \in B$, then from the definition of Θ we have

$$\begin{aligned} |\Theta[\gamma_1(t)] - \Theta[\gamma_2(t)]| &\leq \frac{1}{\Gamma(\varrho)} \int_0^t (t - \wp)^{\varrho-1} |\Psi(\wp, \gamma_1(\wp)) - \Psi(\wp, \gamma_2(\wp))| d\wp \\ &\leq \frac{L_\Psi}{\Gamma(\varrho)} \int_0^t (t - \wp)^{\varrho-1} |\gamma_1(\wp) - \gamma_2(\wp)| d\wp \\ &\leq \frac{L_\Psi b^\varrho}{\Gamma(\varrho + 1)} \|\gamma_1 - \gamma_2\|. \end{aligned}$$

On the other hand,

$$|\Theta[\gamma_1(t)] - \Theta[\gamma_2(t)]| \leq L_\Psi \sigma \|\gamma_1 - \gamma_2\|.$$

Hence, by the Banach contraction principle the considered system (2) has a unique solution in B . \square

6 Numerical scheme

In this section, we present the numerical solutions to the considered models (2).

6.1 Numerical solution of model (2)

To solve model (2) numerically, we apply fractional integral to model (2). Therefore, we have

$$\begin{aligned} \mathcal{X}(t) &= \mathcal{X}(0) + I^\varrho \mathfrak{F}_1(t, \mathcal{X}), \\ \mathcal{Y}(t) &= \mathcal{Y}(0) + I^\varrho \mathfrak{F}_2(t, \mathcal{Y}), \\ \mathcal{Z}(t) &= \mathcal{Z}(0) + I^\varrho \mathfrak{F}_3(t, \mathcal{Z}), \end{aligned}$$

where \mathfrak{F}_1 , \mathfrak{F}_2 , and \mathfrak{F}_3 are as follows:

$$\begin{aligned} \mathfrak{F}_1(t, \mathcal{X}) &= \Xi \mathcal{Y} \mathcal{Z}, \\ \mathfrak{F}_2(t, y) &= \Xi \mathcal{X}^3 - \Xi \mathcal{Y}^3, \\ \mathfrak{F}_3(t, \mathcal{Z}) &= \Omega_\kappa \mathcal{X}^2 + \Pi_\kappa \mathcal{Y}^2 - \eta_\kappa \mathcal{X} \mathcal{Y}. \end{aligned}$$

Replacing t with t_ϖ in the previous equations, we obtain

$$\begin{aligned} \mathcal{X}(t_\varpi) &= \mathcal{X}(0) + I^\varrho \mathfrak{F}_1(t_\varpi, x), \\ \mathcal{Y}(t_\varpi) &= \mathcal{Y}(0) + I^\varrho \mathfrak{F}_2(t_\varpi, y), \\ \mathcal{Z}(t_\varpi) &= \mathcal{Z}(0) + I^\varrho \mathfrak{F}_3(t_\varpi, z), \\ (t_\varpi) &= (0) + I^\varrho \mathfrak{F}_4(t_\varpi, w). \end{aligned}$$

We introduce $t_\varpi = \varpi h$, here h is the step size. Then the above integral equations are rewritten as

$$\begin{aligned} I^\varrho \mathfrak{F}_1(t_\varpi, x) &= h^\varrho \left[k_{\varpi}^\varrho \mathfrak{F}_1(0) + \sum_{j=1}^{\varpi} k_{\varpi-j}^{(\varrho)} \mathfrak{F}_1(t_j, \mathcal{X}_j) \right], \\ I^\varrho \mathfrak{F}_2(t_\varpi, y) &= h^\varrho \left[k_{\varpi}^\varrho \mathfrak{F}_2(0) + \sum_{j=1}^{\varpi} k_{\varpi-j}^{(\varrho)} \mathfrak{F}_2(t_j, \mathcal{Y}_j) \right], \\ I^\varrho \mathfrak{F}_3(t_\varpi, z) &= h^\varrho \left[k_{\varpi}^\varrho \mathfrak{F}_3(0) + \sum_{j=1}^{\varpi} k_{\varpi-j}^{(\varrho)} \mathfrak{F}_3(t_j, \mathcal{Z}_j) \right], \end{aligned}$$

where

$$\mathcal{P}_{\varpi}^\varrho = \frac{(\varpi - 1)^\varrho - \varpi^\varrho(\varpi - \varrho - 1)}{\varrho(2 + \varrho)}.$$

If $n = 1, 2, 3, \dots$, then parameter \mathcal{P} can be expressed as given

$$\mathcal{P}_0^\varrho = \frac{1}{\varrho(2 + \varrho)} \quad \text{and} \quad \mathcal{P}_\varpi^\varrho = \frac{(\varpi - 1)^{\varrho+1} - 2\varpi^{\varrho+1} + (\varpi + 1)^{\varrho+1}}{\varrho(2 + \varrho)}.$$

Next, we transfer the numerical approximations in the previous equation. We obtain the scheme presented below, which is implicit form of the fractional-order chaotic system

$$\begin{aligned} \mathcal{X}(t_\varpi) &= \mathcal{X}(0) + h^\varrho \left[\mathcal{P}_\varpi^\varrho \mathfrak{F}_1(0) + \sum_{j=1}^{\varpi} \mathcal{P}_{\varpi-j}^{(\varrho)} \mathfrak{F}_1(t_j, \mathcal{X}_j) \right], \\ \mathcal{Y}(t_\varpi) &= \mathcal{X}(0) + h^\varrho \left[\mathcal{P}_\varpi^\varrho \mathfrak{F}_2(0) + \sum_{j=1}^{\varpi} \mathcal{P}_{\varpi-j}^{(\varrho)} \mathfrak{F}_2(t_j, \mathcal{Y}_j) \right], \\ \mathcal{Z}(t_\varpi) &= \mathcal{X}(0) + h^\varrho \left[\mathcal{P}_\varpi^\varrho \mathfrak{F}_3(0) + \sum_{j=1}^{\varpi} \mathcal{P}_{\varpi-j}^{(\varrho)} \mathfrak{F}_3(t_j, \mathcal{Z}_j) \right]. \end{aligned}$$

Here we have the relations

$$\begin{aligned} \mathfrak{F}_1(t_j, \mathcal{X}_j) &= \Xi \mathcal{Y}_j \mathcal{Z}_j, \\ \mathfrak{F}_2(t_j, \mathcal{Y}_j) &= \Xi \mathcal{X}_j^3 - \Xi \mathcal{Y}_j^3, \\ \mathfrak{F}_3(t_j, \mathcal{Z}_j) &= \Omega_\kappa \mathcal{X}_j^2 + \Pi_\kappa \mathcal{Y}_j^2 - \eta_\kappa \mathcal{X}_j \mathcal{Y}_j. \end{aligned}$$

Similarly, one can achieve so for model (3).

7 Numerical simulations and discussions

This section presents the numerical illustrations of the numerical scheme used above for the approximation of the solution of system (2). We present the phase projections to analyze the behavior and effects of important parameters and fractional order on the models dynamics (2) and (3). We consider the parameters to be $\Omega_\kappa = 0.2$, $\Pi_\kappa = 0.1$, and $\eta_\kappa = 0.5$. The initial conditions are considered for all the figures as $[\mathcal{X}, \mathcal{Y}, \mathcal{Z}] = [0.1, 0.1, 0.1]$. In Fig. (2) the behaviour of the state variables \mathcal{X} , \mathcal{Y} , \mathcal{X} , \mathcal{Z} , and \mathcal{Y} , \mathcal{Z} in Figs. 2(a), 2(b), and 2(c), respectively. In Fig. 2 the fractional order is selected to be $\varrho = 1$, where the dynamics are observed as in integer-order case. Similarly, in Figs. 3–5 the dynamics of the state variables \mathcal{X} , \mathcal{Y} , \mathcal{X} , \mathcal{Z} , and \mathcal{Y} , \mathcal{Z} demonstrated in subfigures. For Figs. 3, 4, and 5, the fractional orders are considered to be 0.98, 0.94, and 0.90, respectively. It can be seen that the fractional operator has a great impact on the evolution of the oscillator dynamics showing that the system has a limit-cycle attractor. The attractor in the system is realized when the fractional order ϱ becomes 0.90.

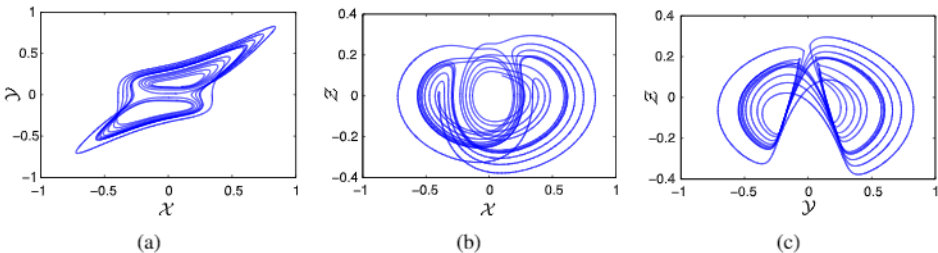


Figure 2. The behavior of state variables \mathcal{X} , \mathcal{Y} of system (2) with fractional order $\varrho = 1$.

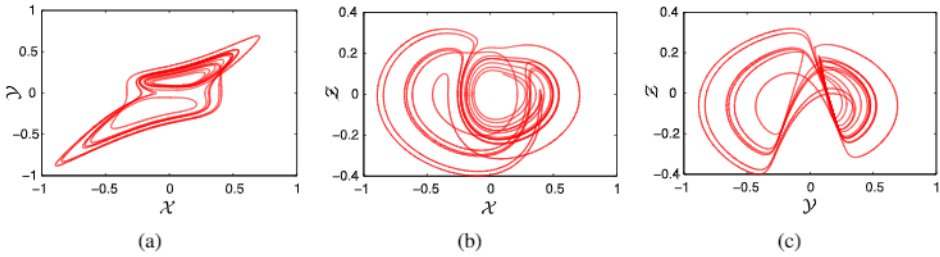


Figure 3. The behavior of state variables of \mathcal{X}, \mathcal{Y} system (2) with fractional order $\varrho = 0.98$.

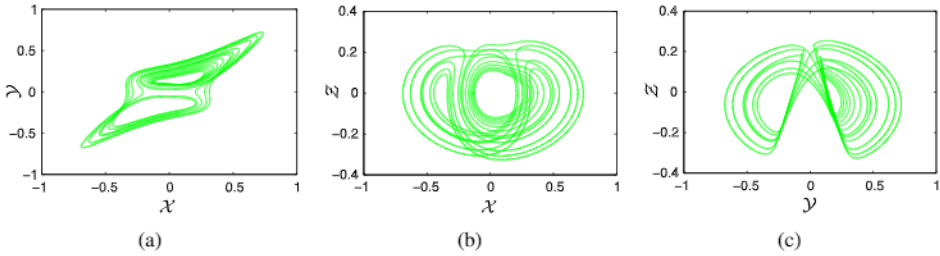


Figure 4. The behavior of state variables \mathcal{X}, \mathcal{Y} of system (2) with fractional order $\varrho = 0.94$.

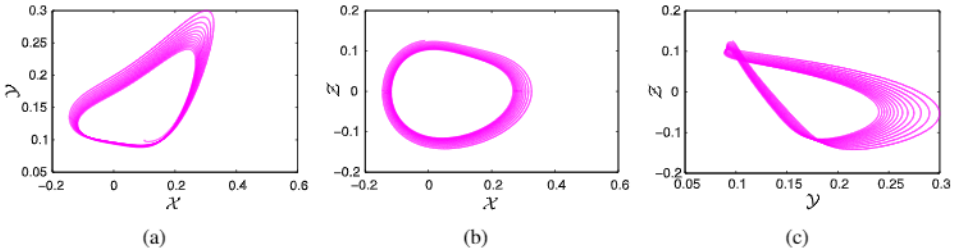


Figure 5. The behavior of state variables \mathcal{X}, \mathcal{Y} of system (2) with fractional order $\varrho = 0.90$.

In Fig. 6 the dynamics of the system state variables \mathcal{Z}, \mathcal{X} and \mathcal{Z}, \mathcal{Y} are projected with different values of the parameter \mathcal{Y} . For the colors blue, red, green, magenta, and cyan, the parameter \mathcal{Y} is supposed to be $-1, -0.5, 0, 0.5,$ and $1,$ respectively. In Fig. 6, ϱ is considered as 1, further, in Fig. 6(a) the ϱ is taken as 0.98, and $\varrho = 0.96$ is selected for Fig. 6(c). These figures show that one can easily control the amplitude of the system state variable \mathcal{Z} with the parameter \mathcal{Y} . The phenomena of controlling the amplitude in a dynamical system are known as offset-boosting control, which is reported in [14]. It is observed that a decrease in ϱ significantly decreases the amplitude faster as compared to the $\varrho = 1,$ which makes these operators more efficient.

The time-series behavior of model (2) is presented in Fig. 7. The oscillations in the classes $\mathcal{X}, \mathcal{Y},$ and \mathcal{Z} are depicted in Figs. 7(a), 7(b), and 7(c), respectively. We see that when ϱ decreases, the system oscillates with lower amplitudes as compared to the higher values of fractional order, showing that the system is evaluating towards a stable region.

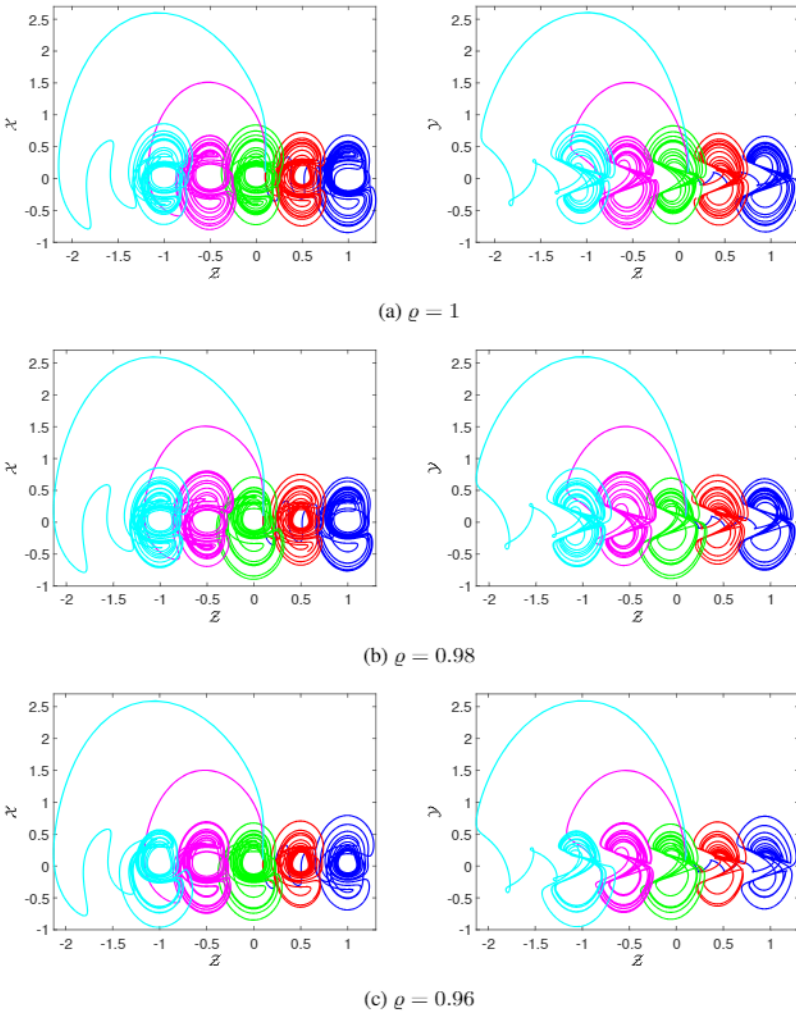


Figure 6. The behavior of state variables Z , X and Z , Y of system (3) with various values of parameter γ .

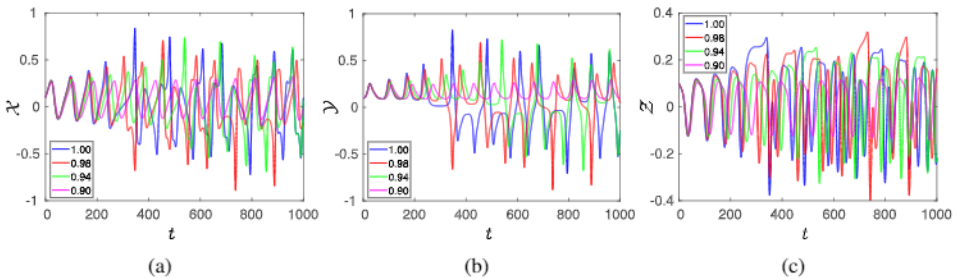


Figure 7. The behavior of state variables X , Y of system (2) with varying fractional order ϱ .

8 Conclusion

In this, we have successfully analyzed a three-dimensional symmetric oscillator with a power-law kernel. The equilibria of the system are studied, which reveals that the system has a line of equilibria. The fixed point theorems guarantee the existence of a unique solution for the considered system. Also, the characteristic equation of the Jacobian of the suggested system has eigenvalues equal to zero, which shows that the considered system is unstable. Further, we investigated the system with a variety of fractional orders, which reveals that when the fractional order decreases, the system tends to converge to a limit-cycle attractor, which is hidden in an integer-order sense. Moreover, the offset-boosting is controlled easily by varying the value of the parameter \mathcal{T} . This system can be further analyzed in the future using different kernels to discover more features of the suggested system.

Acknowledgment. We would like to thank to the referee for his/her valuable comments and suggestions.

References

1. B.R. Andrievsky, N.V. Kuznetsov, G.A. Leonov, A.Yu. Pogromsky, Hidden oscillations in aircraft flight control system with input saturation, *IFAC Proceedings Volumes*, **46**(12):75–79, 2013, <https://doi.org/10.3182/20130703-3-FR-4039.00026>.
2. A. Atangana, D. Baleanu, New fractional derivatives with nonlocal and non-singular kernel: Theory and application to heat transfer model, *Therm. Sci.*, **20**(2):763–769, 2016, <https://doi.org/10.2298/TSCI160111018A>.
3. A. Atangana, K.M. Owolabi, New numerical approach for fractional differential equations, *Math. Model. Nat. Phenom.*, **13**(1):3, 2018, <https://doi.org/10.1051/mmnp/2018010>.
4. M. Caputo, M. Fabrizio, A new definition of fractional derivative without singular kernel, *Progr. Fract. Differ. Appl.*, **1**(2):73–85, 2015.
5. L.O. Chua, C.W. Wu, A. Huang, G.-Q. Zhong, A universal circuit for studying and generating chaos. I. Routes to chaos, *IEEE Trans. Circuits Syst., I, Fundam. Theory Appl.*, **40**(10):732–744, 1993, <https://doi.org/10.1109/81.246149>.
6. A. Durdu, Y. Uyaroglu, A.T. Özcerit, A novel chaotic system for secure communication applications, *Inf. Technol. Control*, **44**(3):271–278, 2015, <https://doi.org/10.5755/j01.itc.44.3.7720>.
7. R. Garrappa, Numerical solution of fractional differential equations: A survey and a software tutorial, *Mathematics*, **6**(2):16, 2018, <https://doi.org/10.3390/math6020016>.
8. N. Heymans, I. Podlubny, Physical interpretation of initial conditions for fractional differential equations with Riemann-Liouville fractional derivatives, *Rheol. Acta*, **45**(5):765–771, 2006, <https://doi.org/10.1007/s00397-005-0043-5>.
9. S.T. Kingni, S. Jafari, H. Simo, P. Wofo, Three-dimensional chaotic autonomous system with only one stable equilibrium: Analysis, circuit design, parameter estimation, control,

- synchronization and its fractional-order form, *Eur. Phys. J. Plus*, **129**(5):76, 2014, <https://doi.org/10.1140/epjp/i2014-14076-4>.
10. S.T. Kingni, V.-T. Pham, S. Jafari, G.R. Kol, P. Wofo, Three-dimensional chaotic autonomous system with a circular equilibrium: analysis, circuit implementation and its fractional-order form, *Circuits Syst. Signal Process.*, **35**(6):1933–1948, 2016, <https://doi.org/10.1007/s00034-016-0259-x>.
 11. K.D. Kucche, S.T. Sutar, Analysis of nonlinear fractional differential equations involving Atangana-Baleanu-Caputo derivative, *Chaos Solitons Fractals*, **143**:110556, 2021, <https://doi.org/10.1016/j.chaos.2020.110556>.
 12. N.V. Kuznetsov, O.A. Kuznetsova, G.A. Leonov, P. Neittaanmäki, M.V. Yuldashev, R.V. Yuldashev, Limitations of the classical phase-locked loop analysis, in *2015 IEEE International Symposium on Circuits and Systems (ISCAS)*, IEEE, 2015, pp. 533–536, <https://doi.org/10.1109/ISCAS.2015.7168688>.
 13. G.A. Leonov, N.V. Kuznetsov, M.A. Kiseleva, E.P. Solovyeva, A.M. Zaretskiy, Hidden oscillations in mathematical model of drilling system actuated by induction motor with a wound rotor, *Nonlinear Dyn.*, **77**(1):277–288, 2014, <https://doi.org/10.1007/s11071-014-1292-6>.
 14. C. Li, J.C. Sprott, Variable-boostable chaotic flows, *Optik*, **127**(22):10389–10398, 2016, <https://doi.org/10.1016/j.ijleo.2016.08.046>.
 15. T. Liu, H. Yan, S. Banerjee, J. Mou, A fractional-order chaotic system with hidden attractor and self-excited attractor and its DSP implementation, *Chaos Solitons Fractals*, **145**:110791, 2021, <https://doi.org/10.1016/j.chaos.2021.110791>.
 16. E.N. Lorenz, Deterministic nonperiodic flow, *Journal of Atmospheric sciences*, **20**(2):130–141, 1963.
 17. G.M. Mahmoud, T.M. Abed-Elhameed, M.E. Ahmed, Generalization of combination–combination synchronization of chaotic n -dimensional fractional-order dynamical systems, *Nonlinear Dyn.*, **83**(4):1885–1893, 2016, <https://doi.org/10.1007/s11071-015-2453-y>.
 18. Z.S. Mostaghim, B.P. Moghaddam, H.S. Haghgozar, Numerical simulation of fractional-order dynamical systems in noisy environments, *Comput. Appl. Math.*, **37**(5):6433–6447, 2018, <https://doi.org/10.1007/s40314-018-0698-z>.
 19. J.M. Munoz-Pacheco, E. Zambrano-Serrano, C. Volos, S. Jafari, J. Kengne, K. Rajagopal, A new fractional-order chaotic system with different families of hidden and self-excited attractors, *Entropy*, **20**(8):564, 2018, <https://doi.org/10.3390/e20080564>.
 20. Z. Odibat, D. Baleanu, Nonlinear dynamics and chaos in fractional differential equations with a new generalized Caputo fractional derivative, *Chin. J. Phys.*, **77**:1003–1014, 2022, <https://doi.org/10.1016/j.cjph.2021.08.018>.
 21. V.-T. Pham, A. Ouannas, C. Volos, T. Kapitaniak, A simple fractional-order chaotic system without equilibrium and its synchronization, *AEU Int. J. Electron. Commun.*, **86**:69–76, 2018, <https://doi.org/10.1016/j.aeue.2018.01.023>.
 22. I. Podlubny, Geometric and physical interpretation of fractional integration and fractional differentiation, *Fract. Calc. Appl. Anal.*, **5**(4):367–386, 2002, <https://arxiv.org/abs/math/0110241>.

23. M.U. Rahman, M. Arfan, W. Deebani, P. Kumam, Z. Shah, Analysis of time-fractional Kawahara equation under Mittag-Leffler power law, *Fractals*, **30**(01):2240021, 2022, <https://doi.org/10.1142/S0218348X22400217>.
24. S. Saifullah, A. Ali, Z.A. Khan, Analysis of nonlinear time-fractional Klein-Gordon equation with power law kernel, *AIMS Math.*, **7**(4):5275–5290, 2022, <https://doi.org/10.3934/math.2022293>.
25. S.S. Sajjadi, D. Baleanu, A. Jajarmi, H.M. Pirouz, A new adaptive synchronization and hyperchaos control of a biological snap oscillator, *Chaos Solitons Fractals*, **138**:109919, 2020, <https://doi.org/10.1016/j.chaos.2020.109919>.
26. N. Sene, Introduction to the fractional-order chaotic system under fractional operator in Caputo sense, *Alexandria Eng. J.*, **60**(4):3997–4014, 2021, <https://doi.org/10.1016/j.aej.2021.02.056>.
27. B. Shiri, G.-C. Wu, D. Baleanu, Terminal value problems for the nonlinear systems of fractional differential equations, *Appl. Numer. Math.*, **170**:162–178, 2021, <https://doi.org/10.1155/2021/6858592>.
28. V.K. Tamba, J. Ramadoss, V.-T. Pham, G. Grassi, O.A. Almatroud, I. Hussain, Symmetric oscillator: Special features, realization, and combination synchronization, *Symmetry*, **13**(11): 2142, 2021, <https://doi.org/10.3390/sym13112142>.
29. Duy Vo Hoang, S. Takougang Kingni, V.-T. Pham, A no-equilibrium hyperchaotic system and its fractional-order form, *Math. Probl. Eng.*, **2017**:3927184, 2017, <https://doi.org/10.1155/2017/3927184>.
30. X. Wang, Y. He, Projective synchronization of fractional order chaotic system based on linear separation, *Phys. Lett. A*, **372**(4):435–441, 2008, <https://doi.org/10.1016/j.physleta.2007.07.053>.
31. L. Zhang, M.U. Rahman, S. Ahmad, M.B. Riaz, F. Jarad, Dynamics of fractional order delay model of coronavirus disease, *AIMS Math.*, **7**(3):4211–4232, 2022, <https://doi.org/10.3934/math.2022234>.